Available online at www.sciencedirect.com
ScienceDirect
Journal of Molecular Catalysis A: Chemical 263 (2007) 115–120
JOURNAL OF MOLECULAR CATALYSIS A: CHEMICAL
www.elsevier.com/locate/molcata

Elucidation of basic properties of mesoporous alumina through the temperature-programmed desorption of carbon dioxide and heterogeneous basic catalysis of mesoporous alumina for the Knoevenagel reaction in supercritical CO_2

Tsunetake Seki [1], Makoto Onaka *

Department of Chemistry, Graduate School of Arts and Sciences, The University of Tokyo, Komaba, Meguro-Ku, Tokyo 153-8902, Japan

Received 15 July 2006; received in revised form 10 August 2006; accepted 18 August 2006
Available online 24 August 2006

Abstract

The temperature-programmed desorption (TPD) of CO_2 has been performed to elucidate the strength and the number of base sites on mesoporous alumina (*meso*Al_2O_3). It was demonstrated that the surface of *meso*Al_2O_3 adsorbs a much smaller amount of CO_2 than those of MgO and conventional γ-Al_2O_3 with irregular pores, but that there exist a small number of strong base sites on *meso*Al_2O_3 that adsorb CO_2 very strongly. The CO_2-TPD results clearly account for the high activity of *meso*Al_2O_3, the low activity of γ-Al_2O_3, and no activity of MgO for a typical base-catalyzed reaction of the Knoevenagel reaction in supercritical CO_2.

Keywords: Mesoporous alumina; Solid base catalyst; CO_2-TPD; Base catalysis; Supercritical CO_2; Knoevenagel reaction

1. Introduction

Mesoporous alumina (*meso*Al_2O_3) is an interesting material with a high surface area and a narrow pore-size distribution in a mesopore region, and has been synthesized using various templates such as polyethylene oxides, carboxylic acids, and tetraalkylammonium salts [1]. While *meso*Al_2O_3 has found its successful application as a catalytic material in a number of reactions involving epoxidation of olefins [2], hydrodechlorination [3], hydrodesulfurization [4], hydrogenation [5], olefin metathesis [6], oxidation of methane to syngas [7], and oxidative dehydrogenation of ethane [8], the utility of *meso*Al_2O_3 as a solid base catalyst and its surface basic property have been scarcely elucidated. We have recently found out that *meso*Al_2O_3 exhibits a highly efficient strong base catalysis for the intramolecular Tishchenko reaction of phthalaldehyde to phthalide even in the acid medium of supercritical CO_2 ($scCO_2$), while conventional γ-Al_2O_3 and a representative solid strong base catalyst of CaO showed a low and no activity, respectively, due to the rapid neutralization by the compressed Lewis acidic molecules of CO_2 [9]. However, the interaction between *meso*Al_2O_3 surface and CO_2 molecules was not elucidated entirely.

Herein, we wish to discuss the properties of base sites on *meso*Al_2O_3 by comparing the profile of temperature-programmed desorption (TPD) of CO_2 and the activity for the Knoevenagel reaction of benzaldehyde (**1**) and ethyl cyanoacetate (**2**) (Scheme 1) with those of MgO and conventional γ-Al_2O_3. The CO_2-TPD analyses gave us novel information about the interaction of CO_2 with *meso*Al_2O_3 surface as well as the strength and the number of base sites on *meso*Al_2O_3, revealing that *meso*Al_2O_3 is an essentially suitable solid base catalyst for the use in $scCO_2$.

2. Experimental

2.1. Catalyst preparations

MgO. To a 3-L beaker containing an excess amount of distilled water (ca. 1 L) was slowly added commercially available high-grade MgO powder (100 g, Merck). The resultant solution was stirred with a mechanical stirrer overnight at room temperature, and boiled in the open air for several hours with

* Corresponding author.
E-mail address: conaka@mail.ecc.u-tokyo.ac.jp (M. Onaka).
[1] Research Fellow of the Japan Society for the Promotion of Science.

1381-1169/$ – see front matter © 2006 Elsevier B.V. All rights reserved.
doi:10.1016/j.molcata.2006.08.049

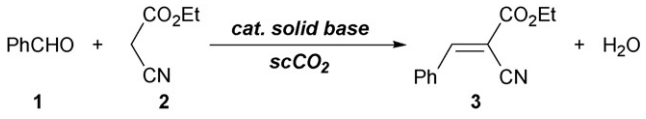

Scheme 1. General reaction equation for the Knoevenagel reaction.

stirring to evaporate water almost completely. The resultant slurry was dried overnight in a furnace to give $Mg(OH)_2$ as white cakes, which was broken into pieces and powdered through a mesh (355–600 μm). Thermal decomposition of the $Mg(OH)_2$ at 773 K under a vacuum (10^{-4} Torr) afforded MgO catalyst.

mesoAl_2O_3. Pure mesoporous alumina (*meso*Al_2O_3) was synthesized according to Davis' report [10]. Into a polypropylene vessel containing a stirring bar were added Al(O-*sec*-Bu)$_3$ (21.9 g, 89.0 mmol, Tokyo Kasei), 1-propanol (120 g, 2.00 mol, Kanto Kagaku), and deionized water (5.15 g, 286 mmol), followed by vigorous stirring at room temperature. After 1 h, a solution of lauric acid (5.40 g, 27.0 mmol, Kanto Kagaku) in 1-propanol (17.5 g, 290 mmol, Kanto Kagaku) was added under vigorous stirring, and the mixture was further stirred vigorously at room temperature for 24 h. The resulting white liquid was placed in a 300-mL autoclave (Taiatsu Techno), and heated at 383 K for 48 h without stirring to afford a white precipitate. The precipitate was washed on a filter paper with a large amount of ethanol, and dried at room temperature under an N_2 flow. The white solid thus obtained was heated from room temperature to 873 K at a ramping rate of 10 K min^{-1} under an N_2 flow, and then calcined under an air flow at 873 K for 5 h to burn out the organic species to give pure *meso*Al_2O_3.

γ-Al_2O_3. JRC-ALO-4, which had been supplied from the Catalysis Society of Japan, was used without any modification. The contents of impurities are as follows: 0.01% Fe_2O_3, 0.01% SiO_2, and 0.01% Na_2O.

2.2. Characterization of the catalysts

N_2 adsorption–desorption measurements were performed at 77 K with a BELSORP 28SA (Bel Japan) using static adsorption procedures. The samples were pretreated under the same condition as employed for the reactions (773 K, 10^{-4} Torr, 2 h) prior to analysis. Adsorption data were analyzed by the Brunauer–Emmett–Teller (BET) method for surface areas and the Dollimore–Heal (DH) method [11] to obtain a pore-size distribution curve.

Powder X-ray diffraction measurement was performed with a MultiFlex (Rigaku) under ambient atmosphere. The sample was pretreated at 773 K at 10^{-4} Torr for 2 h, mounted on an XRD sample cell as fine powder under ambient atmosphere, and analyzed at a current of 40 mA and a voltage of 40 kV in the 2θ range 1–80° with a scanning rate of 1.0° min^{-1}.

2.3. Organic reagents

Benzaldehyde (**1**, Aldrich) and ethyl cyanoacetate (**2**, Kanto Kagaku) were purified by distillation under vacuum, and stored in N_2-filled vials with MS 4A (Wako), which had been activated at 773 K for 2 h under vacuum (10^{-4} Torr) in a vacuum-line apparatus. The vials were placed under very slow N_2 flow to avoid their contacts with humidity as well as the air oxidation of benzaldehyde; nevertheless, benzaldehyde was frequently purified by distillation.

2.4. Temperature-programmed desorption (TPD) of CO_2

The CO_2-TPD was performed in a vacuum-line apparatus equipped with a quadrupole mass spectrometer (QMS 200 F, Pfeiffer Vacuum). Each sample was pretreated at 773 K for 2 h under vacuum. The activated sample (10 mg) was subsequently exposed to 60 Torr of CO_2 at room temperature for 10 min, followed by evacuation at room temperature for 30 min. The TPD was run from room temperature to 1273 K at a heating rate of 10 K min^{-1} under vacuum with the quadrupole mass spectrometer. For γ-Al_2O_3 and *meso*Al_2O_3, the CO_2-TPD was also carried out with an increased amount (50 mg) of the samples, then the pre-evacuation of CO_2 was conducted at 673 K for 5 min just before the TPD-run.

2.5. Reaction procedures

Safety Warning! Operators handling high-pressure equipments for reactions in $scCO_2$ should take proper precautions to minimize the risk of personal injury. The Knoevenagel reaction was performed with an $scCO_2$ reactor system of SCF-Get, SCF-Bpg, and SCF-Sro (Jasco). The detailed reaction procedures were as follows. Into a 10-mL stainless steel autoclave (SUS316, Taiatsu Techno) containing a stirring bar were added freshly distilled benzaldehyde (**1**, 0.1 mL; 0.98 mmol), ethyl cyanoacetate (**2**, 0.1 mL; 0.94 mmol), and a catalyst (30 mg), which had been preactivated at 773 K under vacuum (10^{-4} Torr) for 2 h, in a nitrogen-filled glove bag. Liquid CO_2 cooled to 263 K was introduced into the autoclave, which had been heated to 313 K, using an HPLC pump and the pressure was adjusted to 8.0 ± 0.2 MPa. The resultant mixture was stirred at 313 K at the constant CO_2 pressure of 8.0 ± 0.2 MPa. The autoclave was cooled in an ethanol-dry ice bath, and the pressurized CO_2 was gradually released. The resulting mixture was washed out from the autoclave with CH_2Cl_2. The CH_2Cl_2 slurry was filtered through a Celite pad. Evaporation of the CH_2Cl_2 filtrate gave a crude product, which was dissolved in $CDCl_3$ with Ph_3CH (internal standard substance) and applied to NMR analysis. The amount of the product (**3**) was determined with ^{1}H NMR (270 or 500 MHz) by comparison between the peak area of Ph_3CH and that of the vinyl proton in **3** [12].

The reaction procedures described above gave experimentally reproducible data for several runs.

For comparative purpose, the reaction with MgO was also performed under solvent-free condition in a 10-mL glass flask under N_2 atmosphere.

3. Results and discussion

3.1. Surface area and mesoporosity of the catalysts

The N_2 adsorption–desorption measurements showed that the BET surface areas of MgO, γ-Al_2O_3, and *meso*Al_2O_3 were 267,

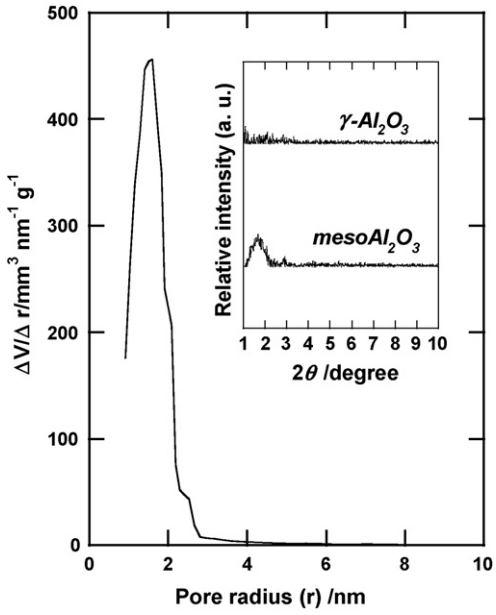

Fig. 1. DH pore-size distribution curve of *meso*Al_2O_3 with XRD patterns of γ-Al_2O_3 and *meso*Al_2O_3.

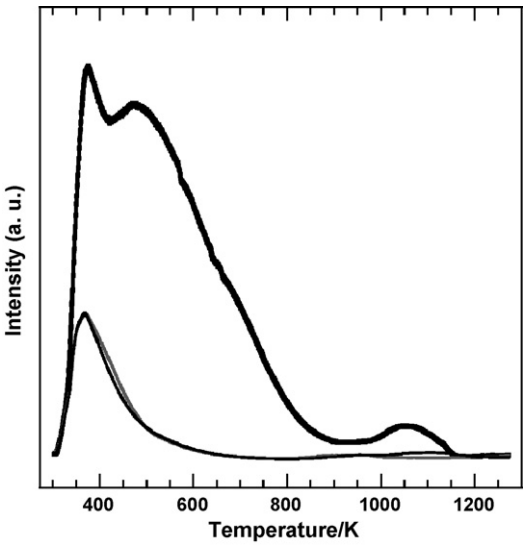

Fig. 2. TPD plots of CO_2 desorbed from 10 mg of MgO (thick black line), γ-Al_2O_3 (thin gray line), and *meso*Al_2O_3 (thin black line) in the temperature range 303–1273 K.

173, and 471 $m^2\ g^{-1}$, respectively, after they had been activated at 773 K for 2 h under vacuum (10^{-4} Torr) prior to the analysis. The measurement also gave the DH pore-size distribution curve of *meso*Al_2O_3, which is shown in Fig. 1. It can be seen from the figure that the *meso*Al_2O_3 possessed a narrow pore size distribution centered at 1.6 nm. The pore volume was 478 $mm^3\ g^{-1}$.

In Fig. 1 are also shown XRD patterns of γ-Al_2O_3 and *meso*Al_2O_3 in the 2θ region 1–10°. The peak at 1–2° for *meso*Al_2O_3 is due to the mesoporous structure, while the similar peak did not appear for γ-Al_2O_3 with irregular pores.

3.2. TPD of CO_2

Fig. 2 shows the TPD plots of CO_2 desorbed from 10 mg of MgO, γ-Al_2O_3, and *meso*Al_2O_3. The pre-evacuation of CO_2 was performed at room temperature for 30 min. The amount of CO_2 desorbed from MgO (4.9 μmol) was far greater than those from γ-Al_2O_3 (0.84 μmol) and *meso*Al_2O_3 (0.83 μmol). The amount of desorbed CO_2 per surface area of MgO was also the highest; the surface area of MgO was 1.5-fold larger than that of γ-Al_2O_3 and 1.8-fold smaller than that of *meso*Al_2O_3. Thus it can be stated that MgO possesses the most CO_2-philic character among the catalysts tested, where we evaluate the "CO_2-philicity" of a material on the basis of the CO_2-adsorbing capacity per surface area.

The amounts of CO_2 desorbed from γ-Al_2O_3 and *meso*Al_2O_3 were almost equal, and far smaller than that of MgO. Note, however, that the amount of desorbed CO_2 per surface area was much smaller for *meso*Al_2O_3 than for γ-Al_2O_3; the surface area of *meso*Al_2O_3 was 2.7-fold larger than that of γ-Al_2O_3. Therefore, it can be concluded that the CO_2-philic character decreases in the order of MgO ≫ γ-Al_2O_3 > *meso*Al_2O_3.

We confirmed a slight difference in the TPD plots in the temperature range 800–1273 K between γ-Al_2O_3 and *meso*Al_2O_3, which indicates that the main CO_2-desorption took place at a higher temperature for *meso*Al_2O_3 than for γ-Al_2O_3 in this temperature region. To further clarify the difference, we performed the TPD experiment with an increased amount of the samples. In Fig. 3 are shown the TPD plots of CO_2 desorbed from 50 mg of γ-Al_2O_3 and *meso*Al_2O_3, where the pre-evacuation of CO_2 was performed at 673 K for 5 min just before the TPD-run; the amounts of desorbed CO_2 in this temperature range were 0.092 and 0.26 μmol for γ-Al_2O_3 and *meso*Al_2O_3, respectively. In this case with an increased amount of the samples is also seen the tendency that the desorption occurred at a higher temperature for *meso*Al_2O_3 than for γ-Al_2O_3. Although both γ-Al_2O_3 and *meso*Al_2O_3 gave the peak in the high temperature region 800–1000 K, only *meso*Al_2O_3 showed the peak centered at a higher temperature of ca. 1100 K. These results clearly indicate

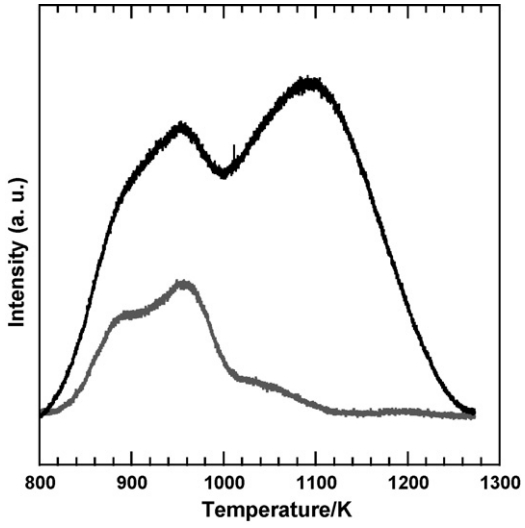

Fig. 3. TPD plots of CO_2 desorbed from 50 mg of γ-Al_2O_3 (gray line) and *meso*Al_2O_3 (black line) in the temperature range 800–1273 K.

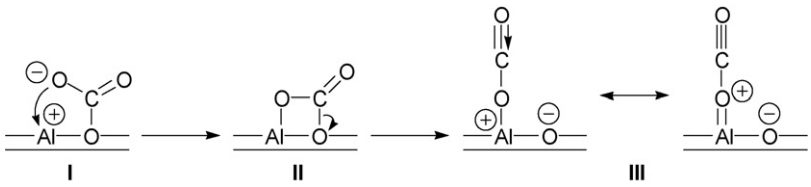

Scheme 2. Migration of adsorbed CO_2 over alumina surface. The electronic structures in **III** were quoted from Ref. [16].

that *meso*Al_2O_3 possesses the base sites with supreme strength that are even stronger than the base sites on γ-Al_2O_3, although there is a possibility that neighboring Lewis acid sites (Al^{3+}) would more or less affect the difference in the TPD profiles, because CO_2 is usually adsorbed on a metal oxide surface in bidentate forms [13].

To sum up, the surface of *meso*Al_2O_3 is essentially less CO_2-philic, but it has a small number of very strong base sites that adsorb acidic CO_2 molecules strongly. We consider that even such strong base sites can easily replace the adsorbed CO_2 with another Brönsted or Lewis acidic molecule (e.g., a reactant in base-catalyzed reactions) that approaches to the base sites, through the action of adjacent Lewis acid sites as shown in Scheme 2.

The similar dynamic behavior of adsorbed CO_2 has been confirmed by Tsuji et al. even over MgO and CaO [14], of which Lewis acid sites (metal cations) are far weaker in acidity than those on alumina [15]. The confirmation of adsorbed species **III** on alumina through infrared spectroscopy by Parkyns [16] also supports the speculation that the same dynamic behavior of adsorbed CO_2 can take place over *meso*Al_2O_3. Moreover, the high activity of *meso*Al_2O_3 for the Tishchenko reaction, which proceeds only by the action of strong base sites (O^{2-}) on metal oxides [17], under $scCO_2$ condition strongly indicates that the strong base sites on *meso*Al_2O_3 are able to release the strongly adsorbed CO_2 by the migration, leading to the constant regeneration of the strong base sites in $scCO_2$ [9].

3.3. The catalytic performances for the Knoevenagel reaction under $scCO_2$ condition

The Knoevenagel reaction is a condensation of an aldehyde or a ketone with an active methylene compound to give the corresponding alkene product together with H_2O [18]. The commonly used base catalysts for Knoevenagel reactions involve secondary amines such as piperidine and Et_2NH, pyridine or pyridine with piperidine (Doebner modification), and metal alkoxides such as NaOEt. These homogeneous catalysts, however, possess several disadvantages in the separation process after the reaction; separation of a product and a catalyst from the resulting solution causes loss of the catalyst and reduction of the product yield. To solve the problems, several researchers have developed solid base catalysts utilizable for Knoevenagel reactions, which, in some cases, are also superior to homogeneous ones in activity and selectivity [19–30].

Both the homogeneous and heterogeneous catalytic reactions have been performed under solvent-free conditions or in conventional organic solvents such as toluene and methanol, and we are unaware of any published reports using $scCO_2$ solvent so far. It is undoubtedly a novel and challenging approach to use acidic $scCO_2$ medium in the base-catalyzed Knoevenagel reaction.

Fig. 4 shows the comparison of the activities of MgO, γ-Al_2O_3, and *meso*Al_2O_3 for the Knoevenagel reaction of **1** with **2** to **3**. Although MgO yielded 0.78 mmol of **3** in 30 min under solvent-free condition, the amount of **3** did not increase in $scCO_2$ from that of **3** formed before starting the reaction under $scCO_2$ condition (i.e., 0.33 mmol) [31]. This was due to the rapid formation of the inactive species of $MgCO_3$ on the surface, and clearly indicates that the representative solid base catalyst of MgO cannot be utilized for base-catalyzed reactions in $scCO_2$.

On the contrary, γ-Al_2O_3 and *meso*Al_2O_3 promoted the reaction even under $scCO_2$ condition. Since the pK_a value of **2** is 9, the base sites stronger than $H_- = 9$ functioned in the compressed CO_2 medium to promote the reaction [15]. It is noteworthy that the activity of *meso*Al_2O_3 was much higher than that of γ-Al_2O_3 at the initial stage of the reaction, demonstrating that *meso*Al_2O_3 is the most suitable solid base catalyst for the Knoevenagel reaction in $scCO_2$ medium; the activity increases in the order of MgO ≪ γ-Al_2O_3 < *meso*Al_2O_3.

It should be noted that there is a good correlation between the activity order for the Knoevenagel reaction in $scCO_2$ and the

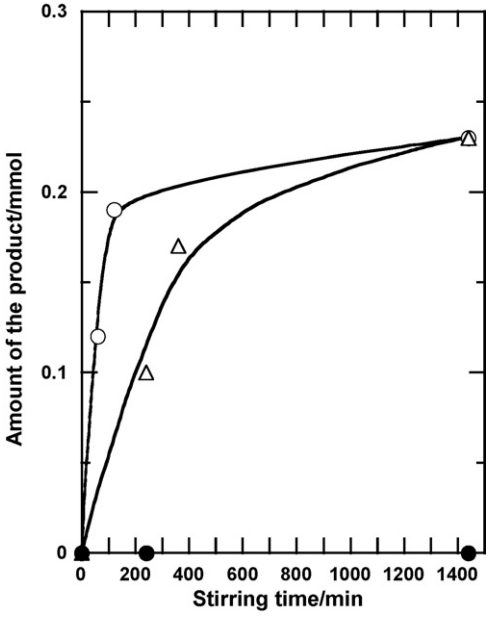

Fig. 4. Variation of the amount of **3** formed over MgO (filled circle), γ-Al_2O_3 (triangle), and *meso*Al_2O_3 (unfilled circle) under $scCO_2$ condition as a function of stirring time (see, Ref. [31]).

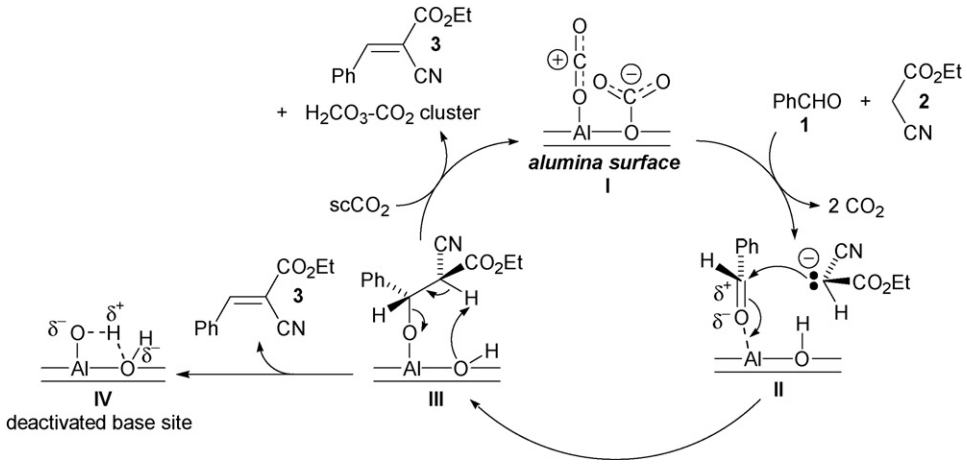

Scheme 3. Plausible mechanism of the Knoevenagel reaction over alumina in $scCO_2$.

results of CO_2-TPD; the less CO_2-philic catalyst with stronger base sites exhibited a higher activity.

3.4. Mechanistic consideration

A plausible mechanism for the Knoevenagel reaction was depicted in Scheme 3 [22]. It can be deduced that the reaction mainly took place through the states **I** → **II** → **III** → **IV**, though some weakly adsorbed H_2O in **IV** might dissolve into $scCO_2$ phase to regenerate **I**. The **IV** is undoubtedly a deactivated state of the active sites, and it can no longer promote the reaction. We consider that the deactivation observed for *meso*Al_2O_3 and γ-Al_2O_3 (Fig. 4) is attributed to the increment of **IV** with the progress of the reaction. Since the equal amount of **3** was finally formed over both the aluminas at 1440 min, almost the same number of active base sites would promote the reaction.

The surface area of *meso*Al_2O_3 was 2.7-fold larger than that of γ-Al_2O_3, nevertheless almost the same amount of CO_2 was desorbed from 10 mg of each alumina in the CO_2-TPD profiles (Fig. 2). This indicates that most of the base sites on the surface of *meso*Al_2O_3 were very weak and released CO_2 molecules by the evacuation at room temperature that was conducted just before carrying out the TPD measurement, and also implies that the numbers of the base sites on *meso*Al_2O_3 and γ-Al_2O_3 that were strong enough to promote the Knoevenagel reaction were almost equal.

Thus the higher activity of *meso*Al_2O_3 at the initial stage of the Knoevenagel reaction in Fig. 4 was not attributed to the higher surface area, but to the nature of active base sites. Although the numbers of active base sites per gram were almost equal for both *meso*Al_2O_3 and γ-Al_2O_3, the density of active base sites, of which strength is enough to promote the Knoevenagel reaction, must be far lower for *meso*Al_2O_3 than for γ-Al_2O_3, considering the much higher surface area of the *meso*Al_2O_3. From the CO_2-TPD results in the temperature range 303–1273 K (Fig. 2), the densities of γ-Al_2O_3 and *meso*Al_2O_3 were estimated as 0.29 and 0.11 nm^{-2}, respectively, where we assume that almost all the base sites releasing CO_2 at this temperature range can promote the Knoevenagel reaction, because the Knoevenagel reaction proceeds by the action of both weak and strong base catalysts [32]. Consequently, even the CO_2 adsorbed on active strong base sites smoothly diffuse over the surface of *meso*Al_2O_3 by the mechanism shown in Scheme 2, due to the large "vacancy" around the sites, when **2** approaches the sites. On the other hand, the CO_2 tightly adsorbed on the active strong base sites of γ-Al_2O_3 are "comparatively jam-packed" because of the high density of active strong base sites, retarding the surface diffusion with each other. As a result, the activation energy for the adsorption of **2** onto the active base sites becomes higher for γ-Al_2O_3 than for *meso*Al_2O_3, which should cause the difference in the activity for the Knoevenagel reaction between γ-Al_2O_3 and *meso*Al_2O_3.

4. Conclusions

It was, for the first time, revealed through the CO_2-TPD experiment that most of the base sites on *meso*Al_2O_3 are weak and do not bond with Lewis acidic molecule of CO_2 strongly, though there are a slight number of very strong base sites that adsorb CO_2 very strongly. There is a good correlation between the CO_2-philic nature of a catalyst and its activity for a typical base-catalyzed reaction of the Knoevenagel reaction in $scCO_2$; a catalyst with the less CO_2-philic character exhibited the higher activity. The CO_2-TPD result also shows the existence of highly strong base sites on the least CO_2-philic material of *meso*Al_2O_3, which adsorb acidic CO_2 molecules very strongly. It must be emphasized that the desorption peak with *meso*Al_2O_3 appeared at a higher temperature than that of conventional γ-Al_2O_3 in the temperature range 800–1273 K. However, it is apparent that those strongest base sites on *meso*Al_2O_3 function even under $scCO_2$ condition, because *meso*Al_2O_3 exhibited high activities for a typical strong base-catalyzed reaction of the Tishchenko reaction [9] as well as the Knoevenagel reaction in $scCO_2$ medium.

Our present results clearly demonstrate that *meso*Al_2O_3 is an essentially appropriate solid base catalyst for various base-catalyzed reactions in $scCO_2$, which is one of the promising

alternatives to conventional organic solvents in view of green chemistry [33].

Acknowledgements

We are grateful to Prof. Dr. Keiichi Tomishige, Dr. Shigeru Kado, and Dr. Takeshi Nobukawa (University of Tsukuba) for the CO_2-TPD measurements.

References

[1] J. Čejka, Appl. Catal. A 254 (2003) 327.
[2] (a) D. Yin, L. Qin, J. Liu, C. Li, Y. Jin, J. Mol. Catal. A 240 (2005) 40;
(b) V.D. Chaube, S. Shylesh, A.P. Singh, J. Mol. Catal. A 241 (2005) 79.
[3] (a) P. Kim, Y. Kim, C. Kim, H. Kim, Y. Park, J.H. Lee, I.K. Song, J. Yi, Catal. Lett. 89 (2003) 185;
(b) P. Kim, Y. Kim, H. Kim, I.K. Song, J. Yi, J. Mol. Catal. A 219 (2004) 87;
(c) P. Kim, Y. Kim, H. Kim, I.K. Song, J. Yi, J. Mol. Catal. A 231 (2005) 247;
(d) P. Kim, J.B. Joo, H. Kim, W. Kim, Y. Kim, I.K. Song, J. Yi, Catal. Lett. 104 (2005) 181.
[4] L. Kaluža, M. Zdražil, N. Žilková, J. Čejka, Catal. Commun. 3 (2002) 151.
[5] (a) L.M. Bronstein, D.M. Chernyshov, R. Karlinsey, J.W. Zwanziger, V.G. Matveeva, E.M. Sulman, G.N. Demidenko, H.-P. Hentze, M. Antonietti, Chem. Mater. 15 (2003) 2623;
(b) S. Valange, A. Derouault, J. Barrault, Z. Gabelica, J. Mol. Catal. A 228 (2005) 255.
[6] (a) M. Onaka, T. Oikawa, Chem. Lett. 31 (2002) 850;
(b) T. Oikawa, T. Ookoshi, T. Tanaka, T. Yamamoto, M. Onaka, Micropor. Mesopor. Mater. 74 (2004) 93;
(c) H. Balcar, R. Hamtil, N. Žilková, J. Čejka, Catal. Lett. 97 (2004) 25;
(d) J. Aguado, J.M. Escola, M.C. Castro, B. Paredes, Appl. Catal. A 284 (2005) 47;
(e) R. Hamtil, N. Žilková, H. Balcar, J. Čejka, Appl. Catal. A 302 (2006) 193;
(f) T. Oikawa, Y. Masui, T. Tanaka, Y. Chujo, M. Onaka, J. Organomet. Chem., in press.
[7] P. Kim, Y. Kim, H. Kim, I.K. Song, J. Yi, Appl. Catal. A 272 (2004) 157.
[8] P. Concepción, M.T. Navarro, T. Blasco, J.M. López Nieto, B. Panzacchi, F. Rey, Catal. Today 96 (2004) 179.
[9] (a) T. Seki, M. Onaka, Chem. Lett. 34 (2005) 262;
(b) T. Seki, M. Onaka, J. Phys. Chem. B 110 (2006) 1240.
[10] F. Vaudry, S. Khodabandeh, M.E. Davis, Chem. Mater. 8 (1996) 1451.
[11] D. Dollimore, G.R. Heal, J. Appl. Chem. 14 (1964) 109.
[12] (a) T. Hayashi, J. Org. Chem. 31 (1966) 3253;
(b) S.-I. Murahashi, T. Naota, H. Taki, M. Mizuno, H. Takaya, S. Komiya, Y. Mizuho, N. Oyasato, M. Hiraoka, M. Hirano, A. Furuoka, J. Am. Chem. Soc. 117 (1995) 12436.
[13] H. Knözinger, Adv. Catal. Relat. Subj. 25 (1976) 184.
[14] H. Tsuji, A. Okamura-Yoshida, T. Shishido, H. Hattori, Langmuir 19 (2003) 8793.
[15] K. Tanabe, M. Misono, Y. Ono, H. Hattori, New Solid Acids and Bases, Kodansha-Elsevier, Tokyo, 1989.
[16] N.D. Parkyns, J. Chem. Soc. A (1969) 410.
[17] (a) K. Tanabe, K. Saito, J. Catal. 35 (1974) 247;
(b) H. Hattori, Chem. Rev. 95 (1995) 537;
(c) T. Seki, H. Tachikawa, T. Yamada, H. Hattori, J. Catal. 217 (2003) 117;
(d) H. Tsuji, H. Hattori, ChemPhysChem 5 (2004) 733.
[18] (a) E. Knoevenagel, Ber. 31 (1898) 2596;
(b) O. Doebner, Ber. 33 (1900) 2140;
(c) G. Jones, Org. React. 15 (1967) 204;
(d) B.K. Wilk, Tetrahedron 53 (1997) 7097.
[19] Anion-exchange resin: R.W. Hein, M.J. Astle, J.R. Shelton, J. Org. Chem. 26 (1961) 4874.
[20] Potassium fluoride: L. Rand, D. Haidukewych, R.J. Dolinski, J. Org. Chem. 31 (1966) 1272.
[21] Alumina: F. Texier-Boullet, A. Foucaud, Tetrahedron Lett. 23 (1982) 4927.
[22] Magnesia: H. Moison, F. Texier-Boullet, A. Foucaud, Tetrahedron 43 (1987) 537.
[23] Alkali-exchanged and alkali-encapsulated zeolites:
(a) A. Corma, V. Fornés, R.M. Martín-Aranda, H. García, J. Primo, Appl. Catal. 59 (1990) 237;
(b) I. Rodriguez, H. Cambon, D. Brunel, M. Laspéras, J. Mol. Catal. A 130 (1998) 195;
(c) C.F. Linares, M.R. Goldwasser, F.J. Machado, A. Rivera, G. Rodríguez-Fuentes, J. Barrault, Micropor. Mesopor. Mater. 41 (2000) 69.
[24] Hydrotalcite: A. Corma, V. Fornés, R.M. Martín-Aranda, F. Rey, J. Catal. 134 (1992) 58.
[25] Amino group-immobilized silica materials:
(a) E. Angeletti, C. Canepa, G. Martinetti, P. Venturello, J. Chem. Soc., Perkin Trans. I (1989) 105;
(b) B.M. Choudary, M.L. Kantam, P. Sreekanth, T. Bandopadhyay, F. Figueras, A. Tuel, J. Mol. Catal. A 142 (1999) 361.
[26] Clay: Y.V. Rao, B.M. Choudary, Synth. Commun. 21 (1991) 1163.
[27] Alkaline and alkaline earth carbonates: M.A. Aramendia, V. Borau, C. Jimenez, J.M. Marinas, F.J. Romero, Chem. Lett. (1995) 279.
[28] Nitridated aluminosilicates and aluminophosphate: S. Ernst, M. Hartmann, S. Sauerbeck, T. Bongers, Appl. Catal. A 200 (2000) 117.
[29] Porous silicate-quaternary ammonium composites: Y. Kubota, Y. Nishizaki, Y. Sugi, Chem. Lett. (2000) 998.
[30] Modified basic microporous titanosilicate ETS-10: Y. Goa, P. Wu, T. Tatsumi, J. Catal. 224 (2004) 107.
[31] The Knoevenagel reaction proceeds very rapidly over MgO and alumina under solvent-free condition, so we could not avoid the "neat" reaction that took place before the introduction of liqCO_2 into the autoclave reactor. The amount of **3** that were formed before starting the reactions in scCO_2 were 0.33, 0.10, and 0.10 mmol for MgO, γ-Al_2O_3, and *meso*Al_2O_3, respectively.
[32] (a) M.B. Smith, J. March, March's Advanced Organic Chemistry: Reactions, Mechanisms, and Structure, 5th ed., Wiley–InterScience, New York, 2001, p. 1225;
(b) M. Zhang, A.-Q. Zhang, Z.-H. Deng, J. Chem. Res. (2005) 69.
[33] (a) A. Baiker, Chem. Rev. 99 (1999) 453;
(b) J.-D. Grunwaldt, R. Wandeler, A. Baiker, Catal. Rev.-Sci. Eng. 45 (2003) 1;
(c) R. Amandi, J. Hyde, M. Poliakoff, in: M. Aresta (Ed.), Carbon Dioxide Recovery and Utilization, Kluwer Academic Publishers, Dordrecht, 2003, p. 169.